

A method to model the cross-polarization of millimeter-wave telescopes using a commercial optical software package

Luca Olmi ^{a b} and Daniel J. Hoppe ^c

^aDept. of Physics, University of Puerto Rico, PO Box 23343
University Station, S. Juan, PR 00931-3343 (USA)

^bIstituto di Radio Astronomia, CNR, Largo E. Fermi 5, I-50125, Firenze (Italy)

^c Jet Propulsion Laboratory, California Institute of Technology, 4800 Oak Grove Drive,
Pasadena, CA 91109-8099 (Daniel.J.Hoppe@jpl.nasa.gov)

ABSTRACT

We discuss the conceptual and practical guidelines of a method to calculate the cross-polarization of a telescope, including its relay optics, using a commercial optical design software, without the need to use complex, slow and expensive Physical Optics programs. These effects are usually negligible at visible and infrared wavelengths but may be of considerable importance at radio wavelengths. Offset reflector antenna configurations, common in the telecommunication industry, and antenna relay optics consisting of offset mirrors, common in millimeter and submillimeter-wave telescopes, result in an increased contribution to the cross-polarization. Polarization measurements are also becoming very important in Radio Astronomy. In fact, dust emission polarimetry and the study of linearly polarized, nonmasing, rotational lines (e.g., CO) with submm telescopes are both powerful diagnostic of magnetic fields in molecular clouds. However, the low average source polarization ($< 2 - 3\%$) requires a careful optimization of the optical design to keep any instrumental polarization contribution from both telescope and relay optics as low as possible in astronomical polarimetry experiments. Likewise, in telecommunication applications polarization separation can be used to effectively double the available bandwidth provided the isolation between the two orthogonal polarization states is sufficient.

Keywords: cross-polarization, optical software, millimeter waves, telescope optics

1. INTRODUCTION

Depolarization effects introduced by reflective optics are vanishingly small when the reflector diameter-to-wavelength ratio becomes very large, i.e., in the Geometric Optics (GO) limit. These effects are thus usually negligible at visible and infrared wavelengths but may be of considerable importance at radio wavelengths. The expression cross-polarization is commonly used to describe how an antenna and its optics alter the polarization state of the feed horn that is used with it. There are then two more contributors, in general, to the cross-polarized field radiated by reflector antennas, as compared to optical instruments. The first, and usually the dominant one is the feed, while the second is the reflector optics itself. In particular, because the antenna relay optics usually consists of offset mirrors and because the feed axis must be oriented towards the reflectors in order to avoid excessive spillover, this system results in an increased contribution to the cross-polarization.

In submillimeter-wave telescopes, all-reflective optics is used to interface the telescope optics to the detectors. However, offset reflector antenna configurations are also common in the telecommunication industry, as they offer several advantages compared to center-fed systems, such as reduced aperture-blocking effects and scattering into the feed. Then, because the (sub)millimeter-wavelength region is also something of an intermediate or crossover region between GO and diffraction methods, it would be important to develop a method to calculate the cross-polarization of the telescope and optics system using a commercial optical design software, rather than complex, slow and expensive Physical Optics programs.

A versatile and quick system to evaluate the cross-polarization introduced by different optical surfaces would be a fundamental tool for the optical designer of submm antennas and their optics used to interface with the

Further author information: E-mail: olmi@naic.edu, Telephone: USA-787-764-0000, ext. 1-7346

focal plane instruments. In fact, the instrumental polarization (IP) introduced by modern submm telescopes is generally $< 0.3\text{--}0.5\%$, which may vary when integrating the main beam area because of the different polarization response of the beam, and because of variation in the field of view if an array of receivers is used. First polarized sidelobes as high as -20dB are not unusual and thus any IP contribution from relay optics should be much less than that. The study of linearly polarized, nonmasing, rotational lines¹ (e.g., CO) with submm telescopes may soon become a powerful and widespread diagnostic of magnetic fields in molecular clouds, offering an alternative to dust emission polarimetry^{2,3,4}. However, the low average line polarization ($< 2 - 3\%$) requires a careful design of the optics used for polarization experiments.

The structure of this paper is thus as follows: in Sect. 2 we discuss some of the systematic effects in (sub)millimeter imaging polarimetry; then, in Sect. 3 we describe the procedure to calculate the cross-polarization with a Physical Optics program, whereas in Sect. 4 we describe how a commercial optical software can be used to calculate the cross-polarization; we finally compare the two methods in Sect. 5.

2. IMAGING POLARIMETRY AT (SUB)MILLIMETER WAVELENGTHS

An important aspect of imaging polarimetry is the removal of IP. Besides to the cross-polarization introduced by the optics, the instrumental term can arise from many other possible sources, such as mis-alignment of the polarizer in the optics path, transmission through a radome or membrane, etc. There are also various instrumental effects that can mimic a polarization signal^{1,5}. Although source polarization can be separated from the instrumental effects at some level, some systematic errors cannot be easily removed from the observations^{6,7}, and thus the design of imaging polarimeters would clearly benefit from an optical system minimizing the variation of the IP across the primary beam and across the field of view (FOV).

As it will be shown in the next sections, accurate polarimetry over broad FOVs may be affected by the optics in several ways. (i) Cross-polarization may be different for distinct points in the FOV. (ii) If wire grids are used to implement either *polarization interleave**, or to separate and detect simultaneously the two orthogonal polarization components of the radiation,⁷ then errors may result from differing co-polarized beam patterns in the two polarizations and from the presence of cross-polarization that can modify the gain of the two parts of the array. In the former case the polarization signal will fluctuate because deviations in instrument pointing cause the two polarized beams to change relative to each other.

Two more effects are worth to be considered. When dealing with extended sources the observing technique of *chopping* from source to a reference, or chop, position can produce systematic error, since the reference position may not be devoid of flux and may be polarized.³ Furthermore, if the telescope auxiliary optics includes large reflecting optics, which have been sized to accept the chopped FOV when using a nutating subreflector (as in the *LMT* case, see Sect. 4), the different cross-polarization at the reference position may add up to the eventual polarized emission from the chop position. In addition, *sidelobe polarization*⁴ can also become a source of systematic error, especially when mapping extended fields in which the source located in the main beam is fainter than sources elsewhere in the FOV. This is particularly true when the cross-polarized beam has a two-lobe or *quasi* two-lobe morphology, as it will be shown later in figures 6 and 7, where the cross-polarization contribution increases dramatically in the sidelobes. In fact, we shall see in Sect. 5 that the cross-polarization has a maximum located beyond the -3 dB point of the main beam, but at the -3 dB point it is only slightly below the maximum. Likewise, when measuring the polarization of point-like sources, pointing errors can cause strong variations of the IP, and thus polarimetry on large millimeter-wave single-dish telescopes may be strongly affected by uncompensated anomalous refraction^{8,9}.

3. CROSS-POLARIZATION WITH A PHYSICAL OPTICS PROGRAM

One of the most widely used methods for the analysis of reflector antennas which includes the effects of diffraction is the Physical Optics (PO, hereafter) method. In this approach each reflecting element is discretized, typically

*The radiation from an assumed *unpolarized* source is split equally onto the two halves on an array, thus alleviating packing problems of the feed-horns at the focal plane.

using triangular facets. The current on each facet is computed using the PO approximation (see, e.g., Balanis¹⁰):

$$\bar{J}_s = 2\hat{n} \times \bar{H}_i \quad (1)$$

where H_i is the incident magnetic field and \hat{n} is a unit vector normal to the surface. These currents then produce a secondary, radiated field which is computed using the radiation integral:

$$\bar{H}(\bar{r}) = -\frac{1}{4\pi} \int_S \left(jk + \frac{1}{R} \right) \hat{R} \times \bar{J}_s(\bar{r}') \frac{e^{-jkR}}{R} ds. \quad (2)$$

here \bar{r} is the observation point, \bar{r}' is the source point, k is the wavenumber, S is the surface of the reflector and R is the source to observation distance:

$$R = |\bar{r} - \bar{r}'|. \quad (3)$$

For a multiple-reflector system the scattering is generally computed in a forward manner, determining the current on the first mirror using the incident field from the feed. The incident field on subsequent mirrors is computed using the radiation integral and the current from the previous mirror. Once the current on the main reflector is determined the final far-field pattern is computed.

PO is a full vector-field diffraction calculation. Both co-polarized and cross-polarized fields are computed exactly from the assumed currents. The currents are approximate in the sense that they are inaccurate near the edge of the reflectors where the PO approximation fails. Fortunately, for most reflector antenna applications the reflectors are large and the incident field is tapered near the edge of the reflectors to reduce spill-over loss and noise contributions. PO is also most accurate in the forward-scatter direction. Again this is not a severe limitation for the analysis of reflector antennas in most cases where the distant sidelobes or rear lobes are unimportant.

In general PO produces computed patterns for the co- and cross-polarized fields that are in excellent agreement with actual measured patterns, particularly in the main beam and first few sidelobe region. PO is also an excellent tool for computing precise values for spillover and the associated noise temperature contribution, whereas ray-based analysis methods are somewhat lacking in this ability. PO can also handle the situation where diffraction effects are critical such as when the feed and reflector, or pairs of reflectors are in the near field of each other or near caustics.

The disadvantage of PO is that it is computationally intensive for multiple reflector systems when the reflectors are large. This is certainly the case for the systems described in this paper where the re-imaging mirrors have dimensions of $\gtrsim 160$ wavelengths and the main reflector is approximately 16700 wavelengths in diameter at the frequency of operation considered here, $\lambda = 3$ mm. These difficulties were overcome through the use of a high-speed parallel computer, running a PO code specifically modified to run efficiently in this computing environment (running time on a SGI2000 computer is about 20 minutes). All PO calculations were carried out for a wavelength of 3 mm, using a feed model consistent with that described later in Section 3.2, Eq. (10). The support struts were not included in the calculation of the cross-polarized component.

4. CROSS-POLARIZATION USING CODE V

4.1. Description of the method

The cross-polarization properties of an optical system can be modeled and investigated using the ray tracing package CODE V.¹¹ One of the the main differences in using a commercial optical design package, as compared to PO programs used in antenna design, consists of the reversed direction of propagation of the radiation. To calculate the cross-polarization (cross-pol, hereafter) the PO program assumes a linearly polarized feed-horn at a given position in the receiver focal plane and then propagates the field through the reimaging and telescope optics. The cross-pol is calculated comparing the X - and Y -components of the far field (assuming Z is set along the optical axis). However, in optical ray tracing programs, with the exception of illumination programs, the source is usually located in the object space and the optical performance is computed at the image (or

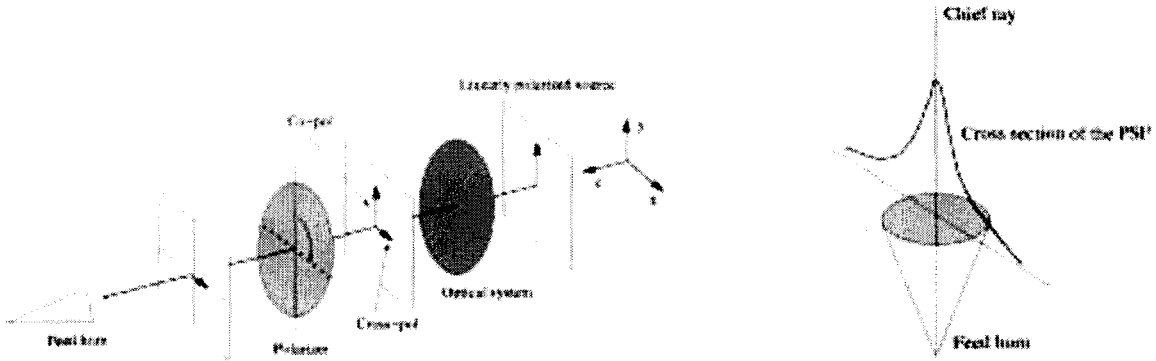


Figure 1. *Left.* Schematic of the method used in CODE V to determine the cross-pol effects on an optical system. The distant source is 100% linearly polarized. In passing through the optical system a cross-polarized component of the field is generated. In the case shown here the (fictitious) linearly polarized filter allows only the cross-polarized component to reach the focal plane. *Right.* In the *coupling method* (see text) the feed-horn in the detector plane is assumed to be aligned with the PSF, i.e. the chief ray and the axis of the feed-horn coincide.

detector) plane. In astronomical telescopes the source is assumed to be located at an infinite distance from the optical system.

Therefore, in order to carry out a meaningful comparison between the two methods, one must specify the polarization state of the *incoming* radiation (i.e. the source on the sky) and the program then models the effects of each interface or optical surface on the polarization state of the traced rays. The co-polar field (or co-pol) at the receiver plane is then taken to be the component of the field which is parallel to the field of the given source, and the cross-polar field is the orthogonal component. Furthermore, the coupling of the Point Spread Function (PSF) with the feed horn must also be considered.

The calculation of the co-pol at the detector plane is done by specifying the linear polarization state of the radiation emitted by the distant 100% polarized source and then inserting a linearly polarized filter just ahead of the image plane (see Fig. 1). Then, according to our previous definition the detector is said to be illuminated by co-polarized radiation when the source and the filter have the same polarization state. However, when the linearly polarized filter is rotated by 90° only the cross-pol component of the field can reach the focal plane. The co-pol and cross-pol components are then compared through their coupling with the feed fields, after they have been properly normalized (see below), and thus one needs to access both amplitude and phase of the field generated by CODE V at the focal plane. The coupling at the focal plane is calculated as¹²:

$$c_{||} = f \left| \int_{\text{horn}} E_{||}(x, y) E_h^*(x, y) dS \right|^2 \quad (4)$$

where $E_{||}(x, y) = A_{||}(x, y) \exp[i\phi_{||}(x, y)]$ is the co-polarized complex field at the focal plane of the telescope, $E_h(x, y) = A_h(x, y) \exp[i\phi_h(x, y)]$ is the feed horn aperture field and f is a normalization factor defined below.

After rotating the linearly polarized filter by 90° the coupling is then:

$$c_{\perp} = \left| \int_{\text{horn}} E_{\perp}(x, y) E_h^*(x, y) dS \right|^2 \quad (5)$$

where $E_{\perp}(x, y) = A_{\perp}(x, y) \exp[i\phi_{\perp}(x, y)]$ is the cross-polarized complex field at the focal plane. In order to determine the proper normalization between the two polarization components, one has to look at the ratio of the average transmittance in each of the polarizer orientations. Then, the intensity results must be scaled by an amount, f , such that:

$$\frac{T_{||}}{T_{\perp}} = \frac{f \int_{\text{horn}} |E_{||}(x, y)|^2 dS}{\int_{\text{horn}} |E_{\perp}(x, y)|^2 dS} \quad (6)$$

where T_{\parallel} and T_{\perp} are the average transmittance for the optical system in the co-pol and cross-pol polarizer configuration, respectively. The two integrals represent the sum of the intensity values in each polarizer configuration.

To calculate the amplitude and phase of the fields in the focal plane CODE V allows access to the complex amplitude for points across the PSF over the image plane. One can then calculate:

$$\begin{cases} A_{\parallel}(x, y) = \left\{ [\text{Re}(E_{\parallel}(x, y))]^2 + [\text{Im}(E_{\parallel}(x, y))]^2 \right\}^{1/2} \\ \phi_{\parallel}(x, y) = \arctan \left[\frac{\text{Im}(E_{\parallel}(x, y))}{\text{Re}(E_{\parallel}(x, y))} \right] \end{cases} \quad (7)$$

which must yield a phase value between 0 and 2π . Likewise, one can obtain $A_{\perp}(x, y)$ and $\phi_{\perp}(x, y)$.

In some cases, such the one we are considering here, the feed horns at the image plane have lenses just ahead of their aperture to compensate for the quadratic phase term in their aperture fields, and thus make the wavefront a planar one. By assuming that the constant phase term in the feed field is zero we will not lose generality and we can then write equations (4) and (5) as:

$$\begin{cases} c_{\parallel} = f \left| \int_{\text{horn}} A_{\parallel}(x, y) A_h(x, y) \exp[i\phi_{\parallel}(x, y)] dS \right|^2 \\ c_{\perp} = \left| \int_{\text{horn}} A_{\perp}(x, y) A_h(x, y) \exp[i\phi_{\perp}(x, y)] dS \right|^2 \end{cases} \quad (8)$$

The cross-pol of the optical system is then easily calculated as:

$$CP = -10 \log \left(\frac{c_{\perp}}{c_{\parallel}} \right) \quad [\text{dB}] \quad (9)$$

We note that all the coupling integrals are calculated assuming that the PSF is aligned with the axis of the feed-horn, as shown in Fig. 1.

However, in the specific case of a null pattern (see sections 5.2 and 5.3) the cross-pol is calculated as the ratio of the two orthogonal field components at the cross-pol peak, after the method has calculated the value and position of the maximum of the cross-polarized lobes (see figures 2, 6 and 7).

4.2. Practical implementation

In CODE V the reflecting properties of the bulk Aluminum reflectors must be first entered, which are usually specified in terms of a proper coating layer and substrate. This means that the complex refractive index of the material must be known at the frequencies of interest. In particular, for proper modeling of metallic reflectors one needs to make sure the coating thickness is thick enough to completely attenuate the radiation before it reaches the substrate. Then, the source polarization properties must be specified, such as: fraction of polarization, polarization type (elliptical, circular or linear), polarization orientation and the “handedness” of the (generally) elliptically polarized beam.

Once these preliminary instructions are completed, a linear polarizer is inserted, just ahead of the image plane, in the optical system to be analysed. Then a PSF calculation is started, using a transform grid size $2^n \times 2^n$, where usually $n = 6$ or greater. The complex PSF output is read into an array, from which the real and imaginary components of the focal plane field are then extracted at the position of interest in the FOV. Next, both amplitude, $A(x, y)$, and phase, $\phi(x, y)$, of the field are calculated and the coupling integral with the horn field can thus be computed using the tangential component of the E -field over the aperture of the horn.

As an example of the application of this method to a real design case we shall use as a baseline telescope design the “*Large Millimeter Telescope*” (*LMT*), a joint USA/Mexico project for the design, fabrication and operation of a 50 m radio telescope in Mexico that will operate in the wavelength range of 1 to 3.4 mm.¹³ The *LMT* will use a 32-element heterodyne focal plane array (FPA) at the relayed focus called *SEQUOIA* (SEcond QUabbin Observatory Imaging Array¹⁴), operating at a wavelength of $\lambda = 3$ mm. The E -field at the aperture

X-polarized source, Y-offset

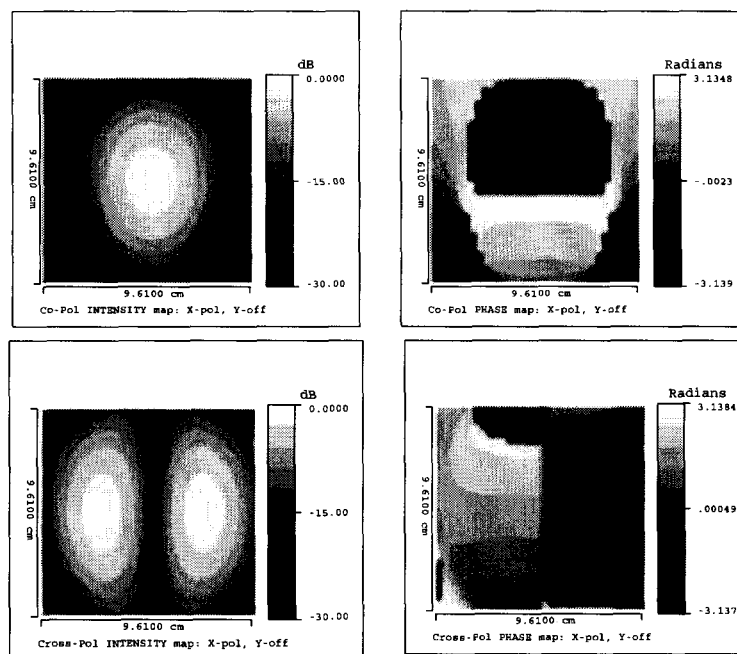


Figure 2. Plots of field intensity and phase at the *Cassegrain* focal plane. Both the co-pol (top) and cross-pol (bottom) components are shown. The horizontal and vertical axes are the X - and Y -axis, respectively (see Fig. 3). Phase is in radians ($-\pi$ to π), whereas the intensity scale is shown in dB below the maximum. The cross-polarization intensity scale has been limited to -30 dB below the maximum and shows the null along the ZY -plane.

of a *SEQUOIA* feed-horn can be written as (N. Erickson, *priv. comm.*):

$$E_h \propto \cos\left(\frac{\pi y}{a}\right) \cos\left(\frac{\pi x}{a}\right), \quad (10)$$

where a represents the x - and y -size of an individual *SEQUOIA* horn. The grid spacing measured on the image plane is chosen so that the Airy disc diameter for $\lambda = 3$ mm spans about 10 grid increments.

This procedure must be run twice, with the linear polarizer initially having the same orientation as the angle of polarization of the incident radiation from the distant source, and then rotated by 90 degrees, while the source polarization remains fixed, to obtain both co-pol and cross-pol as described above. Simultaneously, one must also calculate the transmission of the optical system in both cases to calculate the normalization factor, f . The procedure can be repeated for different positions within the FOV of the FPA, and can also run using different orientations of the source polarization angle (e.g., Y and X).

The method, and especially the calculation of the coupling integrals, was implemented using the internal programming language of CODE V. However, a viable alternative consists of using the internal command, common to several commercial optical software, to calculate the coupling efficiency of a diffraction image into a single-mode optical fiber. One of the most important features of the cross-pol calculation using CODE V, or other similar software, is the ability to incorporate it in a customized optimization procedure^{12,15}.

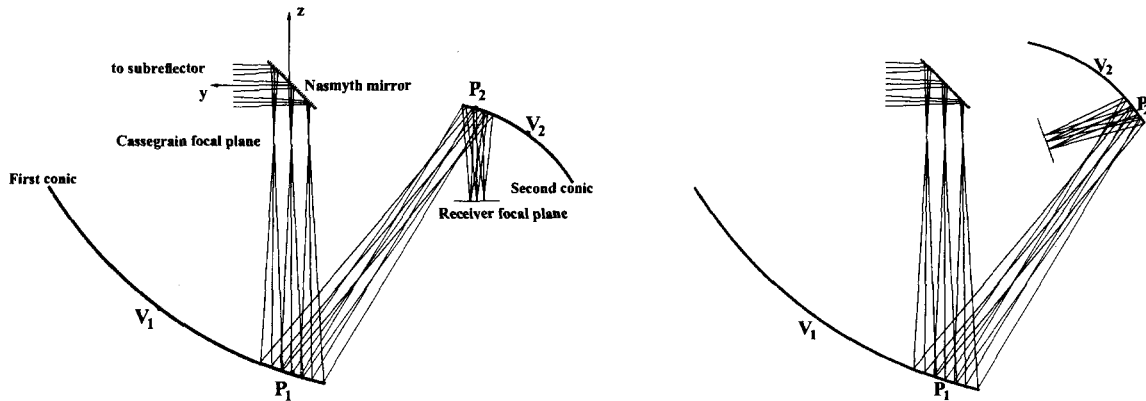


Figure 3. Layout of the two basic relay optics: *Ups* type (left), and *Cpsv* type (right). The *ZY* cut is shown here; the subreflector (not shown) is located to the left of the Nasmyth mirror.¹²

5. COMPARISON OF RESULTS

5.1. Depolarization in offset reflectors

It is well known that the field reflected by a paraboloid contains both X - and Y -polarized components when the incident field is, e.g., Y -polarized, and it is also known that symmetrical cross-pol components are 180° out of phase with one another.¹⁰ In a center-fed paraboloid the cross-pol occurs when the feed radiation is unbalanced, but it has been shown¹⁶ that cross-pol can also originate from the offset between the feed axis and the reflector axis or, more in general, when off-axis surfaces are used in the optical system. In the comparison of cross-pol in center-fed and offset paraboloids Chu & Turrin¹⁶ showed that, owing to cancellation by symmetry, the cross-pol would vanish in the plane of symmetry whereas the plane of asymmetry contains the peak levels of the reflector generated cross-pol (see also Rudge¹⁷).

In the next sections we shall compare the depolarization properties of an offset optical system, using the PO program and the CODE V procedure described above. As a benchmark for this test the optical system designed for the *LMT* will be used. In fact, the installation of either bolometric or heterodyne FPAs on a telescope usually requires the design of an auxiliary “reimaging” or “relay” optics (RO) to convert the focal ratio at the Cassegrain focus to a smaller appropriate focal ratio for the array. Scientific goals generally demand that the telescope be capable of high efficiency imaging over a wide FOV and a broad range of wavelengths. Because the RO is also required to contribute minimally to the overall system temperature the constraints previously mentioned imply a RO design based on large off-axis mirrors, capable of maintaining high image performance over large fields.

5.2. Cassegrain focus

We shall first compare the cross-pol results at the Cassegrain focus of the *LMT*. We considered two different source linear polarizations (or equivalently, two feed-horn polarization states), with the principal linear polarization oriented either along the Y -axis, or orthogonal to it along the X -axis. Radiation patterns were generated, and the cross-pol was calculated, for both polarizations, in the YZ plane of symmetry and in a plane transverse to it. Because the Cassegrain telescope is an optical system with complete rotational symmetry, we do not expect any difference in the cross-pol values. The equivalent angular positions on the sky considered for the test at the Cassegrain focus were $(0, 4')$ and $(4', 0)$. The values of the cross-pol were calculated at the *peak* of the two-lobe cross-polarized PSF, *without* using the coupling method in the case of CODE V. We find that the cross-pol level is -42.9 dB and -46.5 dB as measured by CODE V and the PO program, respectively, for both

Table 1. Values of the cross-pol component in dB relative to the co-pol component, obtained through PO and CODE V, calculated at two positions in the focal plane corresponding to angular offsets $(2', 0')$ (off the YZ plane of symmetry) and $(0', 2')$ (in the plane of symmetry) on the sky. Design types use the definitions of Olmi.¹² At position $(0', 2')$ the values of the cross-pol are calculated at the *peak* of the two-lobe cross-polarized PSF, *without* using the coupling method in the case of CODE V.

Design	Position $(2', 0')$, <i>coupling method</i>				Position $(0', 2')$			
	X-polarized field ^(a)		Y-polarized field ^(a)		X-polarized field ^(a)		Y-polarized field ^(a)	
	PO	CODE V	PO	CODE V	PO	CODE V	PO	CODE V
<i>Ups</i>	-36.4	-41.7	-36.4	-41.7	-35.9	-34.3	-36.9	-34.3
<i>Upd</i>	-29.6	-26.1	-29.7	-29.3	-40.1	-26.5	-40.8	-38.0
<i>Cpsv</i>	-27.6	-20.9	-27.6	-26.8	-42.4	-19.6	-42.8	-42.8
<i>Csv</i>	-27.4	-21.3	-27.6	-26.7	-41.5	-19.4	-42.8	-39.7

(a) Polarization of feed-horn for PO and input beam polarization for CODE V.

off-axis positions and polarizations. We also show an example of cross- and co-polarization patterns obtained with CODE V in Fig. 2.

We note that: (i) there is a 3.6 dB discrepancy between the cross-pol values calculated with CODE V and the PO method (which, at these levels below the co-pol peak, is hardly important in most astronomical applications); (ii) the cross-pol values are the same for each polarization and are independent of the angular offset, as expected. The cross-pol intensity distribution is always dual lobed (symmetric) with a null on axis. The peak cross-pol is about 9.4 arcsec from the co-pol peak, as measured with either CODE V or the PO program. Since the HPBW of the *LMT* is about 14.8 arcsec at $\lambda = 3$ mm, we see that the the cross-pol peak is located beyond the -3 dB point of the main beam, but close to it.

5.3. Receiver focus

In the next phase of this comparison we used several optical designs of RO for single-mode FPAs at millimeter wavelengths, as described in details by Olmi.¹² For the convenience of the reader we summarize here some of their main properties. The designs differ not only in the orientation of the two relay mirrors and the position of their poles, but also in that the phase centers of the Gaussian beams may or may not be at the same position as the geometrical focii of the generating surface.

The specific design type depends on the relative positions of the poles of the two ellipsoids, V_1 and V_2 , on the relative magnitude of the reflection angles (or “symmetry”) and on the positions of the phase centers.¹² In Fig. 3 we show an example of an “Uncrossed” mirror configuration, where the incident rays on the first mirror and the reflected rays on the second mirror, if prolonged, would not cross. The optical system shown in Fig. 3, on the other hand, is commonly defined as a “Crossed” configuration. Two more designs were analysed, one crossed (*Csv*) and one uncrossed (*Upd*) configuration, whose layout however is not shown here.

As we already did in Sect. 5.2 we considered two different source linear polarizations with the principal linear polarization oriented either in the YZ plane along the Y -axis, or orthogonal to it along the X -axis. Contrary to the test performed at the Cassegrain focus, in this case the system exhibits a plane of symmetry, which is the YZ plane (see Fig. 3). Therefore, the cross-pol was calculated, for both polarizations, in the plane of symmetry and in a plane transverse to the plane of symmetry because this plane is expected to show maximum cross-pol for linearly polarized excitation. The equivalent angular positions on the sky were $(0, 2')$ and $(2', 0)$, and the results are listed in Table 1 and are summarized in Fig. 4. The resulting PSFs are shown in figures 6 and 7 for the design type *Cpsv*.

As mentioned previously in Sect. 5.1 the cross-pol patterns in the YZ symmetry plane are theoretically null patterns, and thus very small values for the coupling integrals are expected. In fact, Table 1 lists the cross-pol values obtained with the *coupling method* for the X -offset case only, because CODE V is able to reproduce quite

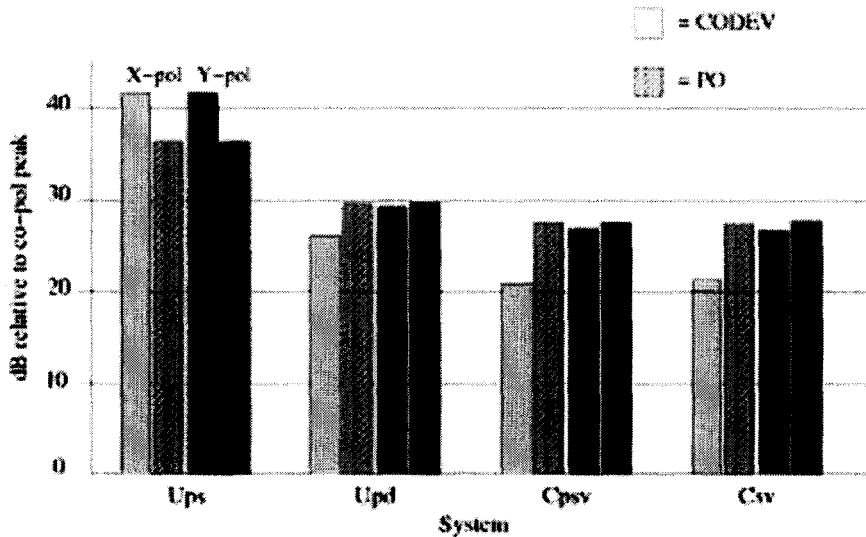


Figure 4. Cross-pol performance for the angular position $(2', 0)$, from Table 1. The light-grey histogram refers to the X-polarization, whereas the dark-grey one shows the Y-polarization results. The histograms with and without the line pattern correspond to the results obtained with the PO program and CODE V, respectively.

well ($\lesssim -200$ dB) the cross-pol null for small offsets along the Y-axis. For this case the PO program predicts an absolute null on axis within the numerical accuracy of the calculation, as expected.

No null is expected for arbitrary decenters off the plane of symmetry, as is the case of the $(2', 0)$ position in the XY plane transverse to the plane of symmetry (figures 6 and 7). In this case the PO program and the CODE V methods show a discrepancy that varies from as little as 0.4 dB to as much as 6.7 dB (see Fig. 4). The difference between the two methods appears to be worst when an X-polarized source is used. Furthermore, in the X-offset case, as shown in Fig. 6(a), CODE V obtains a *quasi* two-lobe morphology, i.e. a two-lobe PSF with a high minimum.

Figures 6 and 7 show that the PSF patterns for the Y-offset case, i.e. for the angular position $(0', 2')$, are virtually identical with polarization either in the plane of symmetry or orthogonal to it. As mentioned earlier, the two-lobe morphology and the central null are expected for small offsets along the Y-axis in the YZ plane of symmetry. The cross-pol maxima are located beyond the -3 dB points of the main co-pol beam (see Fig. 5) and the two-lobe shape is accompanied by a 180° phase reversal across the plane of symmetry (i.e., left to right in figure) in the central part of the phase plot. The cross-pol values listed in Table 1 for this position were obtained at the *peak* of the cross-polarized two-lobe PSF and were calculated comparing the corresponding PSF intensities of the co-pol and the cross-pol beams, i.e. without using the coupling method. Once again, the largest discrepancies between PO and CODE V occur in the case of an X-polarized source, particularly when a *crossed* design is considered. This partial disagreement, which is currently being investigated, may be due to several causes, such as differences between the PO and CODE V cross-pol definitions, differences in the geometrical set-up, convergence of PO, diffraction modeling in CODE V.

ACKNOWLEDGMENTS

This work was partly sponsored by the Advance Research Project Agency, Sensor Technology Office DARPA Order No. C134 Program Code No. 63226E issued by DARPA/CMO under contract No. MDA972-95-C-0004, and by the Puerto Rico NASA Space Grant Consortium. The research described in this paper was in part carried out at the Jet Propulsion Laboratory, California Institute of Technology, under a contract with the National Aeronautics and Space Administration.

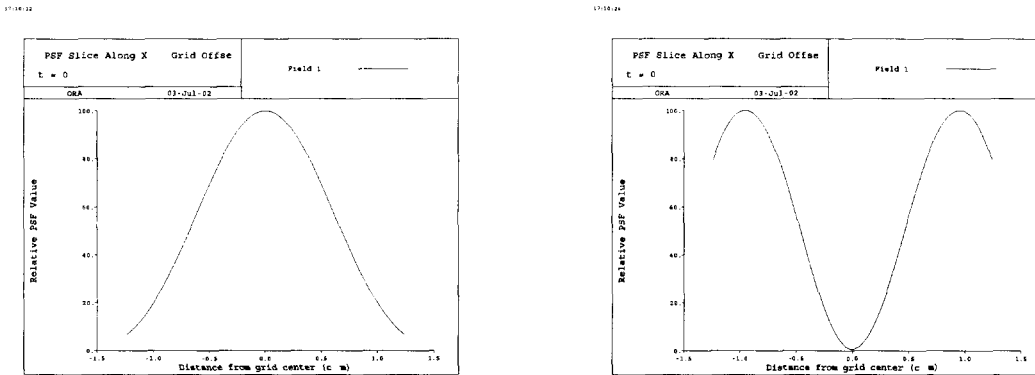
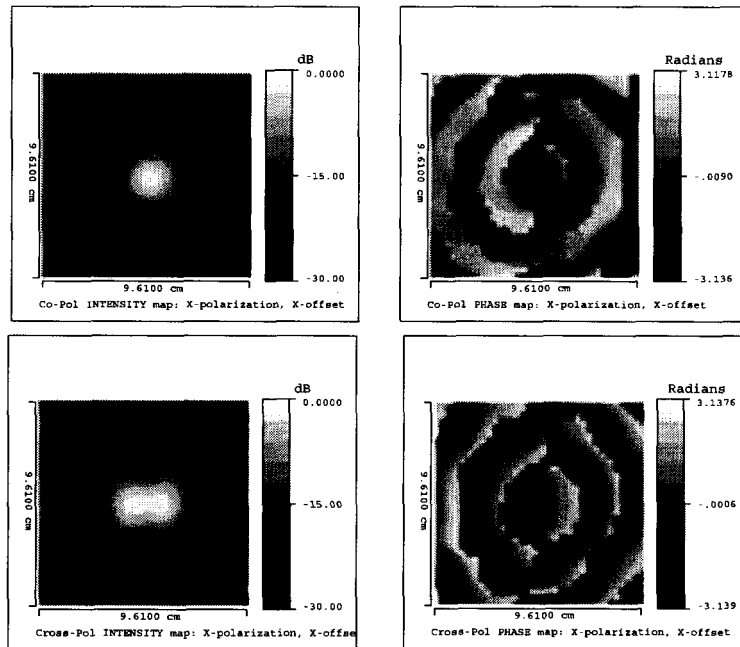


Figure 5. PSF slice along the X -axis of Fig. 7(b), for the co-pol (left) and cross-pol PSF (right).

REFERENCES

1. J. S. Greaves, W. S. Holland, and P. Friberg, "Polarized co emission from molecular clouds," *ApJL* **512**, pp. L139–L142, 1999.
2. J. P. Vallée and P. Bastien, "Extreme infrared ($800\mu\text{m}$) polarimetry of the m17-sw molecular cloud with the jcmt," *Astron. Astrophys.* **313**, pp. 255–268, 1996.
3. B. C. Matthews, C. D. Wilson, and J. D. Fiege, "Magnetic fields in star-forming molecular clouds. ii," *ApJ* **562**, pp. 400–423, 2001.
4. B. C. Matthews, J. D. Fiege, and G. Moriarty-Schieven, "Magnetic fields in star-forming molecular clouds. iii," *ApJ* **569**, pp. 304–321, 2002.
5. D. P. Gonatas, X. D. Wu, G. Novak, and R. H. Hildebrand, "Systematic effects in the measurement of far-infrared linear polarization," *Appl. Opt.* **28**, pp. 1000–1006, 1989.
6. D. A. Schleuning, C. D. Dowell, R. H. Hildebrand, and S. R. Platt, "Hertz, a submillimeter polarimeter," *PASP* **109**, pp. 307–318, 1997.
7. R. H. Hildebrand, J. L. Dotson, C. D. Dowell, G. Novak, D. A. Schleuning, and J. Vaillancourt, "Hertz, an imaging polarimeter," in *Astronomical telescopes and instrumentation*, T. G. Phillips, ed., *SPIE Proceedings Series* **3357**, pp. 289–296, 1998.
8. L. Olmi, "Systematic observations of anomalous refraction at millimeter wavelengths," *Astron. Astrophys.* **374**, pp. 348–357, 2001.
9. L. Olmi, "The effects of the atmosphere," in *NAIC/NRAO School*, S. Stanimirovich, D. R. Altschuler, P. F. Goldsmith, and C. Salter, eds., *ASP Conference Series*, 2002.
10. C. A. Balanis, *Antenna theory*, J. Wiley & Sons, New York, 1997.
11. *Optical Research Associates*, Pasadena, California, 2001.
12. L. Olmi, "The optical design of relay optics for heterodyne millimeter wave focal plane arrays," *International Journal of Infrared and Millimeter Waves* **21**, pp. 365–393, 2000.
13. L. Olmi, "The large millimeter telescope project: overview and optical design," in *Astronomical telescopes and instrumentation*, T. G. Phillips, ed., *SPIE Proceedings Series* **3357**, pp. 186–197, 1998.
14. <http://www.astro.umass.edu/fcrao/instrumentation/sequoia/seq.html>.
15. L. Olmi, "Optical designs for submillimeter-wave spherical-primary (sub)orbital telescopes and novel optimization techniques," in *Astronomical telescopes and instrumentation 2002*, *SPIE Proceedings Series* **4849**, 2002.
16. T.-S. Chu and R. H. Turrin *IEEE Trans. Ant. Prop.* **AP-21**, p. 339, 1973.
17. A. W. Rudge *IEEE Trans. Ant. Prop.* **AP-23**, p. 317, 1975.

(a) X-polarized source, X-offset



(b) X-polarized source, Y-offset

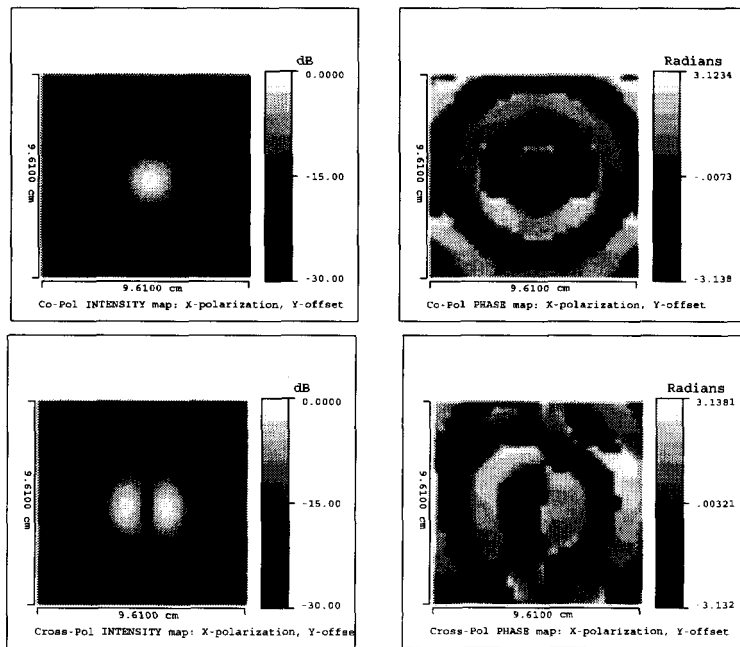
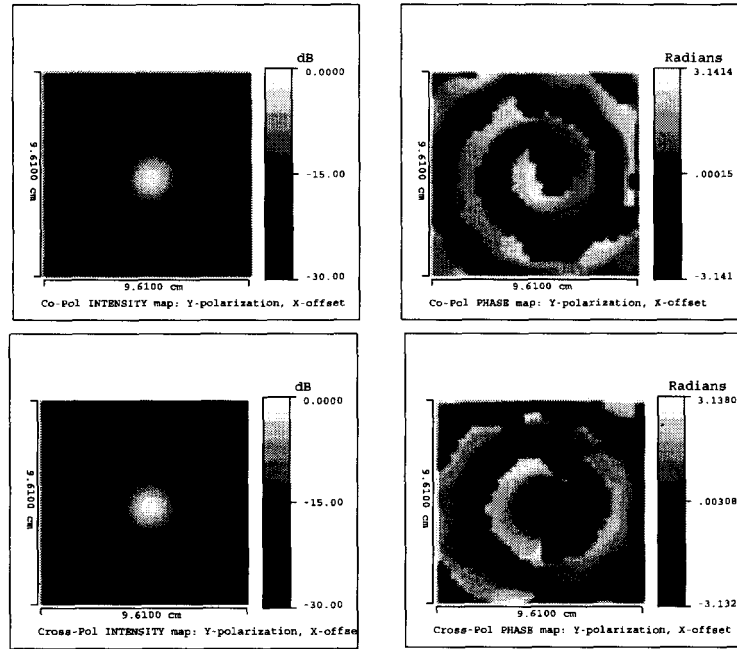


Figure 6. (a) Plots of field intensity and phase at the detector focal plane. Both the co-pol (top) and cross-pol (bottom) components are shown, in the case of an X-polarized source for the *Cpsv* design and for the X-offset angular position $(2', 0)$. Axes and units are the same as in Fig. 2. (b) Same as in (a) for the Y-offset angular position $(0, 2')$.

(a) Y-polarized source, X-offset



(b) Y-polarized source, Y-offset

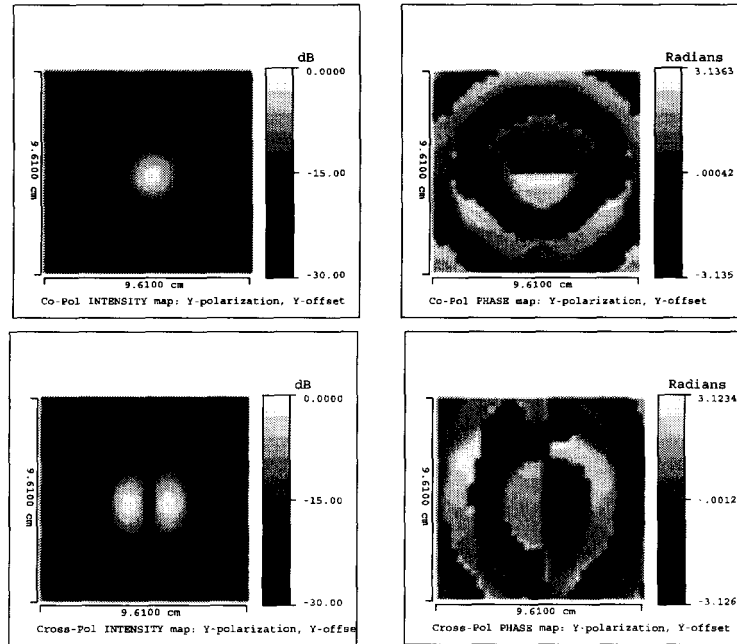


Figure 7. Same as in Fig. 6 for an Y-polarized source.